Figure S1

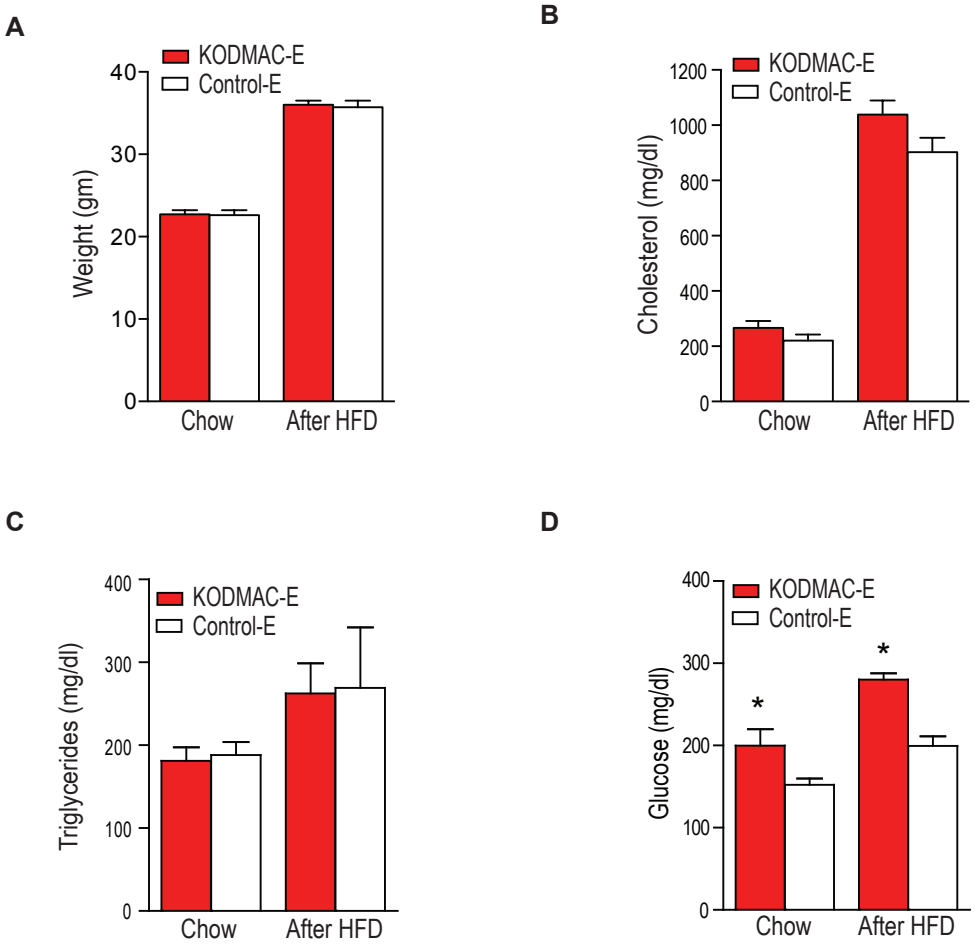
A
KODMAC-E
Control-E
Weight (gm)
40
30
20
10
0
Chow
After HFD
B
KODMAC-E
Control-E
Cholesterol (mg/dl)
1200
1000
800
600
400
200
0
Chow
After HFD
C
KODMAC-E
Control-E
Triglycerides (mg/dl)
400
300
200
100
0
Chow
After HFD
D
KODMAC-E
Control-E
Glucose (mg/dl)
400
300
200
100
0
*
*
Chow
After HFD

Figure S2

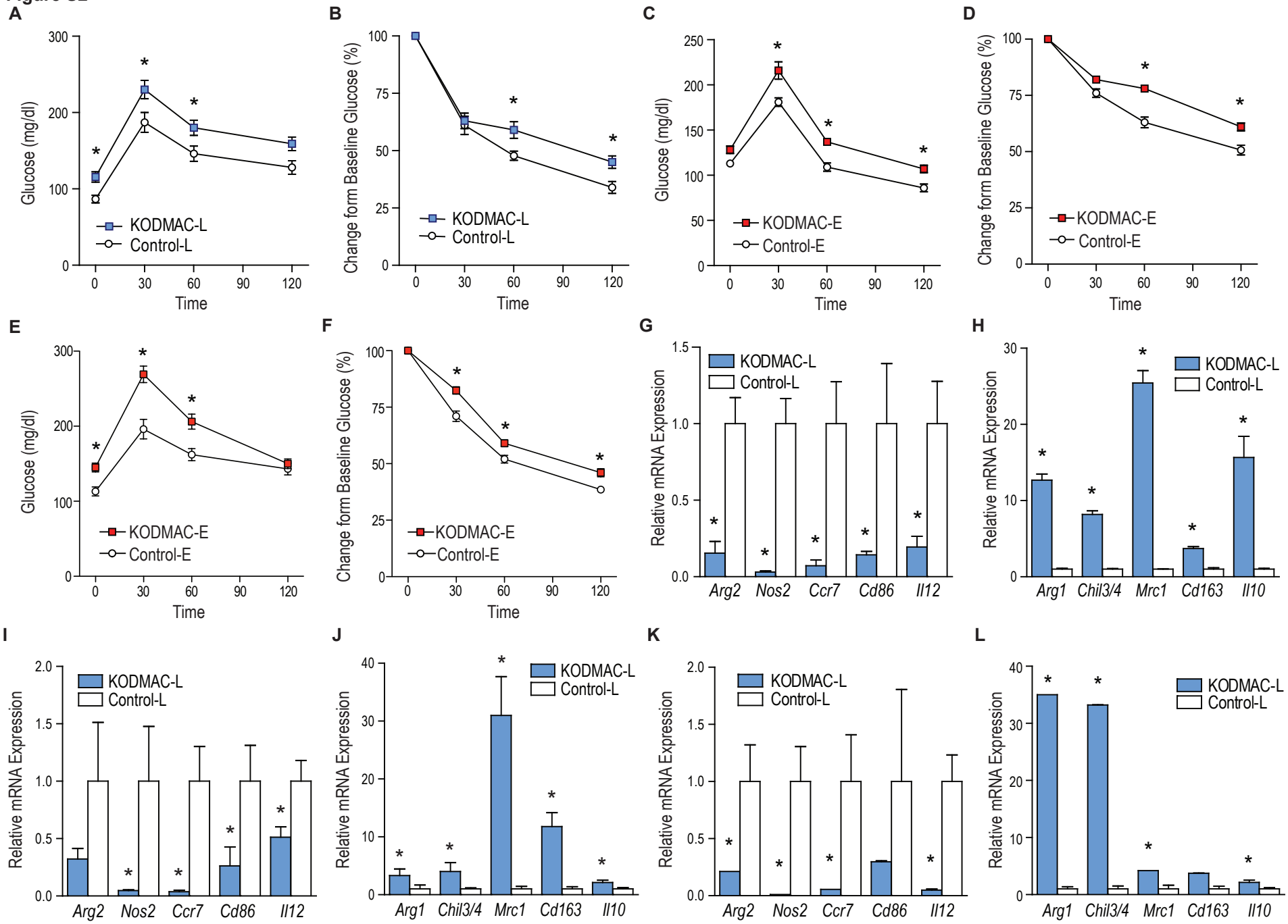
A
B
C
D
E
F
G
H
I
J
K
L
Glucose (mg/dl)
Change form Baseline Glucose (%)
Time
KODMAC-L
Control-L
KODMAC-E
Control-E
Relative mRNA Expression
Arg2
Nos2
Ccr7
Cd86
Il12
Arg1
Chil3/4
Mrc1
Cd163
Il10

Figure S3

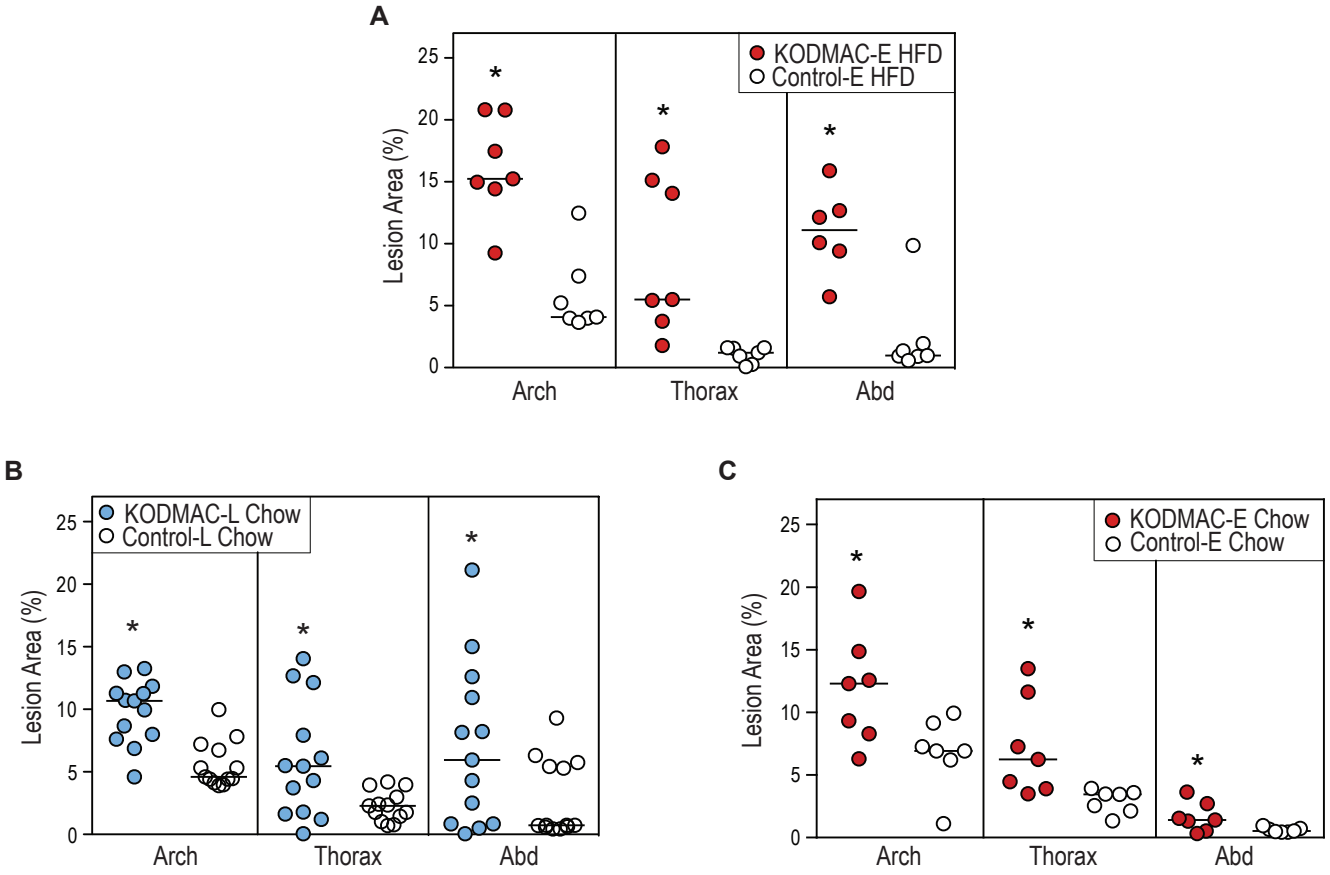
A
KODMAC-E HFD
Control-E HFD
Lesion Area (%)
25
20
15
10
5
0
Arch
Thorax
Abd
B
KODMAC-L Chow
Control-L Chow
Lesion Area (%)
Arch
Thorax
Abd
C
KODMAC-E Chow
Control-E Chow
Lesion Area (%)
Arch
Thorax
Abd

Figure S4

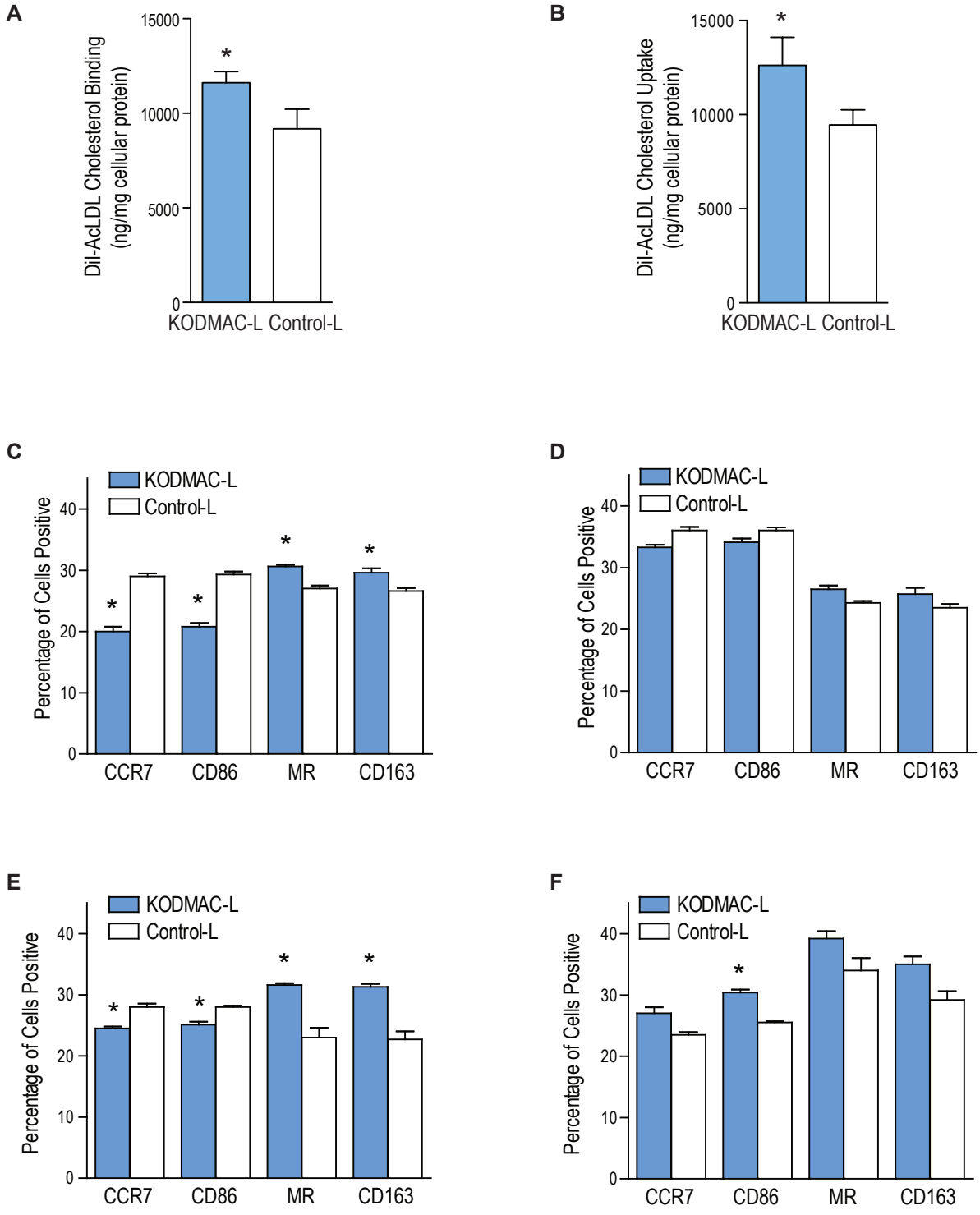
A
Dil-AcLDL Cholesterol Binding (ng/mg cellular protein)
15000
10000
5000
0
*
KODMAC-L Control-L
B
Dil-AcLDL Cholesterol Uptake (ng/mg cellular protein)
15000
10000
5000
0
*
KODMAC-L Control-L
C
KODMAC-L
Control-L
Percentage of Cells Positive
40
30
20
10
0
*
*
*
*
CCR7 CD86 MR CD163
D
KODMAC-L
Control-L
Percentage of Cells Positive
40
30
20
10
0
CCR7 CD86 MR CD163
E
KODMAC-L
Control-L
Percentage of Cells Positive
40
30
20
10
0
*
*
*
*
CCR7 CD86 MR CD163
F
KODMAC-L
Control-L
Percentage of Cells Positive
40
30
20
10
0
*
CCR7 CD86 MR CD163

Figure S5

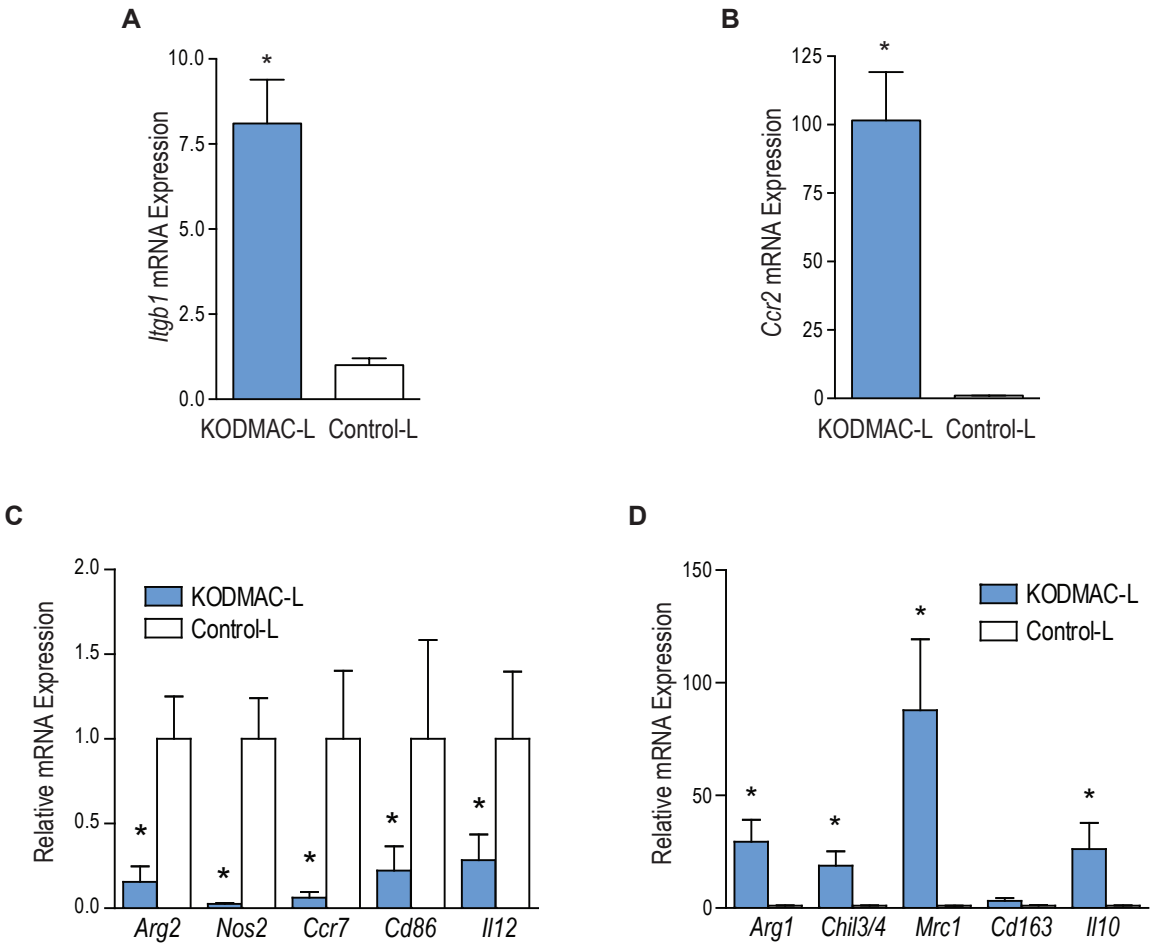
A
Itgb1 mRNA Expression
10.0
7.5
5.0
2.5
0.0
*
KODMAC-L
Control-L
B
Ccr2 mRNA Expression
125
100
75
50
25
0
*
KODMAC-L
Control-L
C
Relative mRNA Expression
2.0
1.5
1.0
0.5
0.0
KODMAC-L
Control-L
*
Arg2
Nos2
Ccr7
Cd86
Il12
D
Relative mRNA Expression
150
100
50
0
KODMAC-L
Control-L
Arg1
Chil3/4
Mrc1
Cd163
Il10

Figure S6

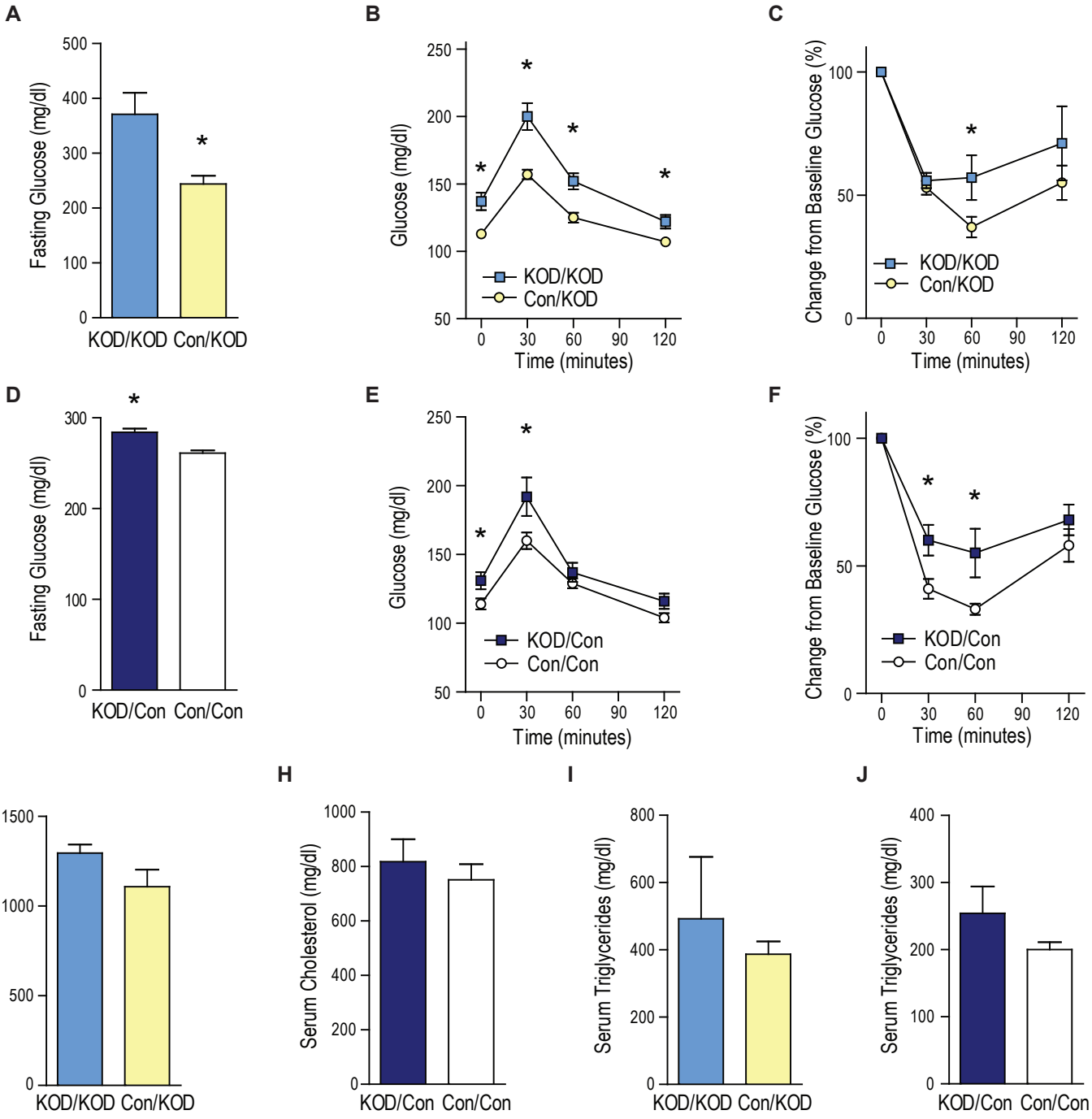
A
Fasting Glucose (mg/dl)
500
400
300
200
100
0
*
KOD/KOD Con/KOD
B
Glucose (mg/dl)
250
200
150
100
50
*
*
*
*
KOD/KOD
Con/KOD
0 30 60 90 120
Time (minutes)
C
Change from Baseline Glucose (%)
100
50
0
*
KOD/KOD
Con/KOD
0 30 60 90 120
Time (minutes)
D
Fasting Glucose (mg/dl)
300
200
100
0
*
KOD/Con Con/Con
E
Glucose (mg/dl)
250
200
150
100
50
*
*
KOD/Con
Con/Con
0 30 60 90 120
Time (minutes)
F
Change from Baseline Glucose (%)
100
50
0
*
*
KOD/Con
Con/Con
0 30 60 90 120
Time (minutes)
G
Serum Cholesterol (mg/dl)
1500
1000
500
0
KOD/KOD Con/KOD
H
Serum Cholesterol (mg/dl)
1000
800
600
400
200
0
KOD/Con Con/Con
I
Serum Triglycerides (mg/dl)
800
600
400
200
0
KOD/KOD Con/KOD
J
Serum Triglycerides (mg/dl)
400
300
200
100
0
KOD/Con Con/Con

Figure S1, related to Figure 1. Body composition and metabolic assessment. KODMAC-E and control-E mice were assessed after 6 wks of chow diet and after an additional 8 wks of high fat diet (HFD). (**A**) Weight (n=16 per group on chow, 7 per group for HFD). After 6 h of fasting in mice on chow diet and after 12 h of fasting in mice on HFD, serum (**B**) cholesterol (n=6 per group), (**C**) triglycerides (n=6 per group), and (**D**) glucose (n=10 per group). **P*<0.05 vs. control-E. Data presented as mean ± SEM.

Figure S2, related to Figure 2. Glucose metabolism and macrophage subtype. In KODMAC-L and control-L mice, (**A**) glucose tolerance test and (**B**) insulin tolerance test after 10 wks of high fat diet (HFD) (n=16 per group). In KODMAC-E and control-E mice, (**C**) glucose tolerance test and (**D**) insulin tolerance test after 6 wks of chow diet (n=7 per group) and (**E**) glucose tolerance test and (**F**) insulin tolerance test after 8 wks of HFD (n=7 per group). From KODMAC-L and control-L mice after 6 weeks of chow, CD11b+ liver macrophages, bone-marrow-derived macrophages, and peritoneal macrophages were isolated. qRT-PCR analysis of relative mRNA expression of (**G**) M1 macrophage genes *Arg2*, *Nos2*, *Ccr7*, *Cd86*, and *Il12* and of (**H**) M2 macrophage genes *Arg1*, *Chil3/4*, *Mrc1*, *Cd163*, and *Il10* from liver macrophages (n=4 per group). qRT-PCR analysis of relative mRNA expression of (**I**) M1 macrophage genes and (**J**) M2 macrophage genes from bone-marrow-derived macrophages (n=4 per group). qRT-PCR analysis of relative mRNA expression of (**K**) M1 macrophage genes and (**L**) M2 macrophage genes from peritoneal macrophages (n=4 per group). Expression normalized to *Mprl32*. **P*<0.05 vs. control. Data presented as mean ± SEM.

Figure S3, related to Figure 3. Atherosclerosis. In KODMAC-E and control-E mice, (**A**) atherosclerotic plaque area by en face technique of pinned aortas after 8 wks of high fat diet (n=7 per group). In (**B**) KODMAC-L and control-L mice (n=13 per group) and (**C**) KODMAC-E and control-E mice (n=7 per group), atherosclerotic plaque area after 1 yr on chow diet. **P*<0.05 vs. control. Data presented as mean ± SEM.

Figure S4, related to Figure 4. ER stress and macrophage subtype. In peritoneal macrophages from KODMAC-L and control-L mice after 10 wks of high fat diet, (**A**) cholesterol binding and (**B**) cholesterol uptake after DiI-acetylated-LDL stimulation (n=4 per group). In CD11b+ peritoneal macrophages from KODMAC-L and control-L mice after 6 weeks on chow, flow cytometry analysis of M1 macrophage markers CCR7 and CD86 and M2 macrophage markers CD163 and MR after incubation (**C**) without or (**D**) with ER stress inhibitor PBA or after incubation (**E**) without or (**F**) with ER stress inducer and SERCA inhibitor Thapsigargin (n=3 per group). **P*<0.05 vs. control-L. Data presented as mean ± SEM.

Figure S5, related to Figure 5. Monocyte subtype and function. In CD11b+ peripheral monocytes from KODMAC-L and control-L mice, qRT-PCR analysis of (**A**) *Itgb1* (β1-integrin) (n=6 per group), (**B**) *Ccr2* (n=6 per group), (**C**) M1

macrophage genes *Arg2*, *Nos2*, *Ccr7*, *Cd86*, and *Il12* (n=4 per group), and (**D**) M2 macrophage genes *Arg1*, *Chil3/4*, *Mrc1*, *Cd163*, and *Il10* (n=4 per group) normalized to *Mprl32*. **P*<0.05 vs. control-L. Data presented as mean ± SEM.

Figure S6, related to Figure 6. Metabolic parameters after transplantation. All assessments were performed in fasting mice after HFD. In irradiated KODMAC-L mice transplanted with BM from KODMAC-L (KOD/KOD) or control-L (Con/KOD) animals, (**A**) fasting plasma glucose, (**B**) glucose tolerance test, and (**C**) insulin tolerance test. In irradiated control-L mice transplanted with BM from KODMAC-L (KOD/Con) or control-L (Con/Con) animals, (**D**) fasting plasma glucose, (**E**) glucose tolerance test, and (**F**) insulin tolerance test. Fasting serum cholesterol and triglycerides in (**G**, **H**) KOD/KOD and Con/KOD mice and in (**I,J**) KOD/Con and Con/Con mice. (n=7 KOD/KOD, 11 Con/KOD, 9 KOD/Con, 10 Con/Con) **P*<0.05 vs. KOD/KOD or Con/Con. Data presented as mean ± SEM.

Supplemental Experimental Procedures

Experimental models

For bone marrow transplantation, BM cells were isolated from the femurs and tibias of 8-10 week old KODMAC-L and control-L mice on chow diet by flushing the bones with cold PBS (Schneider et al., 2006). Total bone marrow was washed, triturated using a 24-gauge needle (Benson Dickson), collected by centrifugation at 1250 rpm for 4 min, and diluted with PBS. After lysis of erythrocytes using 0.05% sodium azide, cells were counted to obtain a defined concentration of unfractionated bone marrow. Eight-week-old KODMAC-L and control-L recipient mice on chow diet were lethally irradiated with 10 Gy from a cesium 137γ cell irradiator. Within 6 h after irradiation, recipients were reconstituted with ~5 × 10^6 donor marrow cells via a single injection. The donor marrow was allowed to repopulate for 6 weeks after transplantation prior to assessment. The resultant null allele was detected by genotyping of DNA from blood (Qiagen Blood Kit). For estimating engraftment, total bone marrow was isolated from the femurs and tibias from C57BL/6-TgN (ACTbEGFP) (GFP) mice in the *Ldlr*$^{-/-}$ background in parallel for each transplant experiment. The marrow was processed as described and ~5 × 10^6 cells of unfractionated bone marrow in PBS were injected into a cohort of *Ldlr*$^{-/-}$ mice. FACS quantification of the percentage of GFP positivity in peripheral leukocytes revealed engraftment of 80%–92%. Recipient mice were placed on 6 weeks of chow, followed by 10 weeks of HFD with metabolic assessment before and after HFD and atherosclerosis assessment after HFD.

Metabolic assessment

For glucose and insulin tolerance tests**,** mice were fasted for 6 or 12 h for chow and HFD, respectively, before peritoneal injection with 10% D-glucose (1 g/kg, Hospira) or human regular insulin (0.75 U/kg, Humulin R, Eli Lilly) in procedures separated by at least 1 week. Tail vein blood was assayed for glucose at baseline and at 30, 60, and 120 minutes after injection using a blood glucose meter (Bernal-Mizrachi et al., 2003). Hyperinsulinemic euglycemic clamps were performed as we previously described (Funai et al., 2013). A jugular and femoral catheter were implanted, tunneled subcutaneously, and exteriorized at the back of the neck. Five days after surgery, animals were fasted overnight and glucose turnover was measured in the basal state and during a hyperinsulinemic euglycemic clamp in conscious mice. For the basal phase, blood samples were obtained, then 3-[^{3}H]D-glucose (American Radiolabeled Chemicals) was infused (0.05 μCi/min) with a Y-connector. One hour after the start of the tracer infusion, a second basal blood sample was taken for measurement of glucose concentration and tracer-specific activity to estimate rate of appearance (Ra) or rate of disappearance (R_d) ($R_a = R_d$ for the basal phase). For the clamp phase, infusion of 3-[^{3}H]D-glucose was replaced with a solution that contained 3-[^{3}H]D-glucose (0.05 μCi/min) and regular human insulin (Humulin R, Eli Lilly) at 2.5 mU/kg/min (with 50 mU/kg prime). Through a second port on the Y-connector, 20% D-glucose was infused at an adjustable rate to maintain blood glucose at 120 mg/dl. After 75 min of steady state blood glucose at 120 mg/dl, a final blood sample was taken to estimate R_a and R_d during the clamp phase ($R_a \neq R_d$ for the

clamp phase). Insulin-stimulated whole body glucose disposal rate (GDR) is calculated as the ratio of the clamp [^{3}H] glucose infusion rate to the specific activity of plasma glucose during the final 30 min of the euglycemic clamp. Percentage of baseline hepatic glucose production, an indicator of liver insulin sensitivity, was calculated from R_a-clamp and R_a-basal values [(R_a-basal – R_a-clamp) / R_a-basal]. For hepatic insulin signaling, human insulin (5 U/kg) was injected into the inferior vena cava after a 6 h fast. Liver was isolated and snap frozen in liquid nitrogen at 2 min. Tissue homogenates were immunoblotted for phospho-AKT (Ser473) (Cell Signaling) (Odegaard et al., 2008).

Hepatocyte isolation and macrophage co-culture

For the macrophage-hepatocyte co-culture, primary hepatocytes were isolated and cultured using Invitrogen liver media and reagents. Livers of anesthetized 8-week-old control-L mice were perfused with hepatocyte perfusion media with collagenase (Invitrogen) via catheterization of the inferior vena cava. Digested livers were then resected and dissociated in liver wash buffer. Hepatocytes were allowed to recover for 24 h on collagen-coated plates in hepatozyme with 10% FBS (Invitrogen) (Newberry et al., 2003). Macrophages were cultured for 24 h as described above prior to seeding onto hepatocyte cultures at a 1:2 macrophage:hepatocyte ratio and co-culturing for a further 18 h. Alternatively, hepatocytes were cultured for 18 h with KODMAC-L or control-L macrophage media only. For liver cholesterol quantification, samples were homogenized and extracted with chloroform/methanol (1:2 v/v), dried under nitrogen, and reconstituted for enzymatic assays using commercial reagents (Thermo Electron

Corp). Results were normalized to protein content of the homogenate (Newberry et al., 2003).

Flow cytometry

Monocyte and macrophage cell surface marker analysis was performed using a FACStar Plus as we previously described (Oh et al., 2012; Riek et al., 2012). After isolation, including CD11b selection with microbeads, cells were resuspended in flow cytometry buffer (2% BSA and 0.1% sodium azide in PBS), and at least 10^5 cells were analyzed for each sample. There was no difference in results after blocking with 200 µg/ml IgG, so this was not routinely performed. Monocytes or macrophages were stained with PerCP-CY5.5-conjugated anti-Ly6c (1:100, E-Bioscience), PE-conjugated anti-CCR2 (1:100, R&D Biosystems), and FITC-conjugated anti-CD115 (1:100, E-Bioscience) for monocyte marker expression; APC-eFluor780-conjugated anti-CCR7 (1:100, E-Bioscience) and eFluor450-conjugated anti-CD86 (1:100, E-Bioscience) for M1 macrophage marker expression and Cy5.5-conjugated anti-CD163 (1:100, Bioss USA) and Alexa700-conjugated anti-MR (1:100, R&D Systems) for M2 macrophage marker expression.

Murine atherosclerotic lesions

For atherosclerosis assays, aortae were prepared using the *en face* technique (Bernal-Mizrachi et al., 2005; Tordjman et al., 2001). Results were reported as percentage involvement of the intimal surface for three regions of the aorta as analyzed using Image J. The percentage of involvement of the intimal surface area is reported for the arch (encompassing the surface from the aortic valve to

the left subclavian artery), the thoracic aorta (extending to the final intercostal artery), and the abdominal aorta (to the ileal bifurcation). To detect the co-localization of differentiated macrophages with cholesterol deposition in the atherosclerotic plaque in the proximal aorta, mice were anesthetized and exsanguinated, the heart and aortic arch were perfused, then tissues were removed en bloc and frozen immediately in Tissue Freezing Medium (Triangle Biomedical Sciences). For each sample, 64 sections were made on a cryostat beginning just caudal to the aortic sinus and extending into the proximal aorta at 10 μm intervals. Slides were fixed with 4% Formalin and 6 cryosections of the aortic root were stained with antibodies specific for CCR7 (M1 marker) or MR (M2 marker) (1:200 for both, Santa Cruz Biotechnology) and adipocyte differentiation-related protein (ADRP, 1:250, American Research Product) following the manufacturer's recommendations as we previously described (Oh et al., 2012). Plaque M1 or M2 macrophages were assessed as the percentage of total plaque area (determined based on adjacent H&E-stained sections) with staining for CCR7 or MR. Lipid colocalization with M1 or M2 macrophages was measured by the percentage of total ADRP staining area colocalizing with staining for CCR7 or MR.

Cellular cholesterol metabolism

Foam cell formation, cholesterol binding and uptake, cholesterol ester formation, and cholesterol efflux were assessed as we previously described (Oh et al., 2012; Oh et al., 2009). Foam cell formation was assessed by fixing macrophage slides with 5% paraformaldehyde for 15 min and staining with Oil-red-O. Cellular

lipids (total and free cholesterol) were extracted with chloroform/methanol (1:2 v/v), dried under nitrogen, and reconstituted for enzymatic assays using commercial reagents (Thermo Electron Corp).(Oh et al., 2012) Results were normalized to total cell protein concentrations. To assess cholesterol binding and uptake, cells in 12-well plates were incubated for 6 h with 10 μg/mL oxidized LDL (oxLDL) labeled with 1,1'-dioctadecyl-3,3,3',3'-tetramethyl indocarbocyanine percholate (DiI; Invitrogen) at 4^{o} (binding) or 37^{o} (binding and uptake). Cholesterol uptake was calculated by subtracting the cholesterol measured at 4^{o}C (binding only) from the cholesterol measured at 37^{o}C (uptake and binding). Cholesterol uptake was also performed in some macrophages after incubation for 24 h with 10 uM of the CaMKII inhibitor, N-[2-[N-(4-Chlorocinnamyl)-N-methylaminomethyl]phenyl]-N-(2-hydroxyethyl)-4-methoxybenzenesulfonamide phosphate salt (KN93, Sigma), and DiI-oxLDL was added for the final 6 h of culture. For cholesterol ester, macrophages were incubated with oxLDL (200 μg/mL) with ^{3}H oleic acid (0.1 mM) (American Radiolabeled Chemicals Inc.) for 6 h. Lipids were extracted, dried under nitrogen, and separated by TLC. Spots representing the cholesterol ester and free oleic acid were counted. Results were normalized to total cell protein concentrations. For cholesterol efflux, macrophages were incubated for 24 h with oxLDL (100 μg/mL) preincubated with 5 mCi of ^{3}H cholesterol (American Radiolabeled Chemical, Inc.). Six h following replacement of media with serum-free media containing apolipoprotein AI (25μg/mL) or HDL (50 μg/mL), supernatant and cells were assessed for radioactivity. Efflux of ^{3}H cholesterol from the cells into the medium was

calculated as percent of total ^{3}H cholesterol incorporated in the cells after incubation.

SERCA2b activity

The calcium transport assay for measuring SERCA2b activity was performed as we previously described (Funai et al., 2013). ER fractions were isolated by differential centrifugation in macrophages. The assay mixture contained 100 mM KCl, 30 mM imidazole-histidine (pH 6.8), 5 mM MgCl2, 5 mM ATP, 5 mM (COOK)2, 5 mM NaN3, 1 μM Rethenium Red, and 50 μM CaCl2 (1 μCi/μmol [45Ca]CaCl2; American Radiolabeled Chemicals). The reaction was started by the addition of ER fractions containing 150 μg protein for 15 minutes in a 37°C water bath, stopped by the addition of 0.15 M KCl and 1 mM LaCl3, and filtered through a 0.2-μm HT Tuffryn membrane (Pall Corp). SERCA-independent calcium transport was quantified in the presence of 10 μM thapsigargin.

Monocyte adhesion and migration

96-well-plates were coated with fibronectin (Sigma) overnight. Monocytes (0.1 x10^{5} cells/plate) were added to fibronectin-coated plates and incubated for 4 hours at 37°C. Adhered cells were then washed, fixed in formaldehyde, and stained with Crystal violet. Well absorbance was read at 585 nm. Transwell migration assays were performed with 5 μm Costar polycarbonate filters as previously described (Riek et al., 2013; Riek et al., 2012). Membranes and 12-well plates were coated with fibronectin (5 μl/mL; Sigma) overnight at 4°. Monocytes (0.3 × 10^{5} cells/well) were added to the upper chamber, and MCP-1 (100 ng/well; Sigma) in 0.8% agarose solution was added to the lower chamber

to stimulate migration. Cells migrating into the lower chamber after 8 h of incubation were manually counted.

Monocyte cholesterol transport

Cholesterol-d_7 [25,26,26,26,27,27,27-$^2H_7$] was synthesized by Sigma-Aldrich and contained 99 atom % deuterium. It was dissolved in warm ethanol, added dropwise to 20% Intralipid, and passed through a 1.2 μm particulate filter to yield an emulsion containing 4 mg/ml cholesterol-d_7 as described previously (Bosner et al., 1993; Lin et al., 2009). The sterile material was stored at 2-8ºC for one year with a resulting increase of greater than 10-fold in thiobarbituric acid reactive substances reflecting fatty acid oxidation (Lin et al., 2006). We incubated monocytes with stably-labeled, non-naturally-occurring cholesterol-d_7 (Bosner et al., 1999; Bosner et al., 1993) for 6 h and then infused them into recipient mice. Plasma from infused mice was collected at 6, 12, and 24 h. Aortas were isolated and cleaned with PBS 24 h after cholesterol-d_7-labeled monocyte infusion. Neutral lipids were extracted in chloroform/methanol (1:2, v/v) and dried and then saponified with ethanolic potassium hydroxide (Bosner et al., 1993), extracted with petroleum ether, dried, and taken up in toluene. Underivatized sterols were injected into a Thermo TSQ 8000 GC/MS/MS instrument, separated on a 30 m x 0.25 mm i.d. x 0.25 μ film thickness RTX 200 column, subjected to electron ionization at 70 ev and ions at *m/z* 386 (M^+) and 393 $(M+7)^+$ were acquired in single-quadrupole mode. The assay was calibrated by standard mixtures of cholesterol/cholesterol-d_7. Monocyte cholesterol enrichment was reported as the mole ratio of cholesterol-d_7 ester/natural cholesterol. Aortic cholesterol ester

enrichment was reported as the relative ratio between aorta mole ratio of cholesterol-d_7 ester/natural cholesterol to the plasma ratio. For two-photon microscopy of explanted aortas, peripheral blood monocytes were isolated by CD11b microbeads and pooled from 4 mice for each infusion, then cultured in vitamin D-deficient media plus 1,25$(OH)_2D_3$ (10^{-8} mol/L) and DiI-oxLDL (10 μg/ml) for 6 h. Cells were then washed with cold PBS, spun down, and resuspended in 200 μl PBS for intravenous infusion of ~10^6 cells into recipient mice. Recipient mice received daily DiI-oxLDL-cholesterol-incubated monocyte infusions for 3 d prior to aortic explant. Recipient mice were anesthetized with Avertin (Avertin prepared with 2,2,2 Tribromethanol and 2 Methylbutanol, Sigma-Aldrich, St. Louis, MO). The aorta was cut at the branches of common iliac arteries and aortic root. The branches of aorta were cut at 1-2 mm from the aorta. The aorta was placed in CO_2-independent medium (Gibco) and stained with Alexa Fluor 594 anti-mouse CD31 Ab (endothelial marker, Biolegend) at 1:5 in PBS at room temperature for 30 min. After two washes with PBS, the aorta was placed in a chamber filled with PBS for two-photon microscopy. Optical sections were acquired by taking 60 sequential z steps at 2.5 μm spacing. Each plane represents an image of 220 μm (x) by 240 μm (y) (at 2 pixels/μm). Imaging was performed using a custom-built video-rate 2P microscope equipped with a Chameleon Vision II Ti:Sapphire laser (Coherent) (Zinselmeyer et al., 2009). A laser excitation wavelength of 1000 nm was found to produce simultaneous fluorescence excitation of nanoparticles, Emission was passed through 495nm, 540 nm and 605 nm dichroic mirrors placed in series and detected as red (>560

nm), green (510 to 560 nm), and blue (<510nm) channels by four head-on multi-alkali photomultiplier tubes. Image reconstruction smoothing, contrast enhancement, multidimensional rendering and depth measurements were performed with Imaris (Bitplane).

Gene expression

For qRT-PCR, total RNA (1 μg) was treated with DNase and reverse transcribed using Superscript II (Invitrogen) with oligo-dT as primer. PCR was performed with the GeneAmp 7000 Sequence Detection System using the TaqMan or SYBR® Green reagent kit (Applied Biosystems). RNA not subjected to reverse transcription was included in each assay as negative control. We used the following mouse oligonucleotides: *Vdr* forward, 5'-CGC CAG ACC AGA GTT CTT TTG-3', *Vdr* reverse, '5-ACA GAT CCG AGG CAC ATT CC -3' *Vdr* probe, 5'-/56-FAM/CTG TTC ACC TGC CCC TTC AAT GGA GAT /36-TAMSp/-3'; *Cyp24a1* forward '5-CTGCCCCATTGACAAAAGGC-3', *Cyp24a1* reverse 5'-CTAACCGTCGGTCATCAGC-3'; *Pck1* forward, 5'-CTGGATGAAGTTTGATGCCC-3', *Pck1* reverse, 5'-TGTCTTCACTGAGGTGCCAG-3'; *G6pc* forward, 5'-TCGGAGACTGGTTCAACCTC-3', *G6pc* reverse, 5'-TCACAGGTGACAGGGAACTG-3'; *Itbg1* forward, 5'-GGTATGACGCTGCAGACTATCC-3', *Itbg1* reverse, 5'-CAGTACGACACCTACCACGG-3'; *Ccr2* forward, 5'-TGGCTGTGTTTGCTTCTGTC-3' Ccr2 reverse 5'-TCTCACTGCCCTATGCCTCT-3'; *Il10* forward, 5'-

CTGCCCCATTGACAAAAGGC-3'; *Il10* reverse, 5'- CTAACCGTCGGTC ATCAGC-3'; *Il12* forward, 5'-CTGCCCCATTGACAAAAGGC-3'; *Il12* reverse, 5'-CTAACCGTCGGTCATCAGC-3'; *Arg1* forward, 5'- CAG AAG AAT GGA AGA GTC AG-3'; *Arg1* reverse, 5'-CAG ATA TGC AGG GAG TCA CC -3'; *Arg2* forward, 5'-TGA TTG GCA AAA GGC AGA GG -3'; *Arg2* reverse, 5'-CTA GGA GTA GGA AGG TGG TC -3'; *Nos* forward, 5'-TGC ATG GAC CAG TAT AAG GCA AGC-3'; *Nos* reverse, 5'- GCT TCT GGT CGA TGT CAT GAG CAA-3'; *Ccr7* forward, 5'-TCCTTCTCATCAGCAAGCTGT -3'; *Ccr7* reverse, 5'-GAGGCAGCCCAGGTCCTTGAAG-3'; *Cd86* forward, 5'-GGGGGATCCATGGGCTTGGCAATCCTTAT -3'; *Cd86* reverse, 5'-TCGGGTGACCTTGCTTAGACGTGCAGG -3'; *Chil3/4* forward, 5'-CTGATCTATGCCTTTGCTGG -3'; *Chil3/4* reverse, 5'-CACAGATTCTTCCTCAAAAGC -3'; *Mrc1* forward, 5'-CTCGTGGATCTCCGTGACAC -3'; *Mrc1* reverse, 5'-ATGGAAGAGACCTTCAGCTAC -3'; *Cd163* forward, 5'-ATGGGCTAACTCCAGCGCCG -3'; *Cd163* reverse, 5'-GATCCATCTGAGCAGGTCACTCCA-3'; *Mrpl32* RNA forward, 5'- AAG CGA AAC TGG CGG AAA ; *Mrpl32* RNA reverse, 5'- GAT CTG GCC CTT GAA CCT TCT ; *Mrpl32* forward, 5'-AAGCGAAACTGGCGGAAAC-3', *Mrpl32* reverse, 5'-GATCTGGCCCTTGAACCTTCT-3', *Mrpl32* probe, 5'-HEX-CAGAGGCATTGACAACAGGGTGCG-BH-3'. All assays were done in triplicate. Results are expressed as relative expression of mRNA normalized to mouse ribosomal protein *Mrpl32.*

Immunoblotting and immunoprecipitation

Western blotting was performed by standard techniques. Cell lysates were analyzed by Western blot for: VDR (1:500, Santa Cruz); ER stress proteins [pPERK and PERK (1:1000, Cell Signaling), CHOP (1:500, Santa Cruz)]; proteins involved in cholesterol signaling [JNKp (1:1000, Cell Signaling), PPARγ,SR-A1, CD36 (1:500, Santa Cruz)]; SERCA2 (1:500, ABcam); and pCAMKII and CAMKII (1:1000, Cell Signaling), and β-actin (1:1000, Cell Signaling) was used as a loading control. For immunoprecipitation, macrophage lysates from control-L mice after 6 wks of chow were incubated with monoclonal anti-VDR (1:250, ABcam) or normal rabbit serum overnight, then blotted overnight with anti-SERCA2 (10 μg, ABcam) as previously described (Zhao and Simpson, 2010).

Supplemental References

Bernal-Mizrachi, C., Gates, A.C., Weng, S., Imamura, T., Knutsen, R.H., DeSantis, P., Coleman, T., Townsend, R.R., Muglia, L.J., and Semenkovich, C.F. (2005). Vascular respiratory uncoupling increases blood pressure and atherosclerosis. Nature *435*, 502-506.

Bernal-Mizrachi, C., Weng, S., Feng, C., Finck, B.N., Knutsen, R.H., Leone, T.C., Coleman, T., Mecham, R.P., Kelly, D.P., and Semenkovich, C.F. (2003). Dexamethasone induction of hypertension and diabetes is PPAR-alpha dependent in LDL receptor-null mice. Nat Med *9*, 1069-1075.

Bosner, M.S., Lange, L.G., Stenson, W.F., and Ostlund, R.E., Jr. (1999). Percent cholesterol absorption in normal women and men quantified with dual stable isotopic tracers and negative ion mass spectrometry. J Lipid Res *40*, 302-308.

Bosner, M.S., Ostlund, R.E., Jr., Osofisan, O., Grosklos, J., Fritschle, C., and Lange, L.G. (1993). Assessment of percent cholesterol absorption in humans with stable isotopes. J Lipid Res *34*, 1047-1053.

Funai, K., Song, H., Yin, L., Lodhi, I.J., Wei, X., Yoshino, J., Coleman, T., and Semenkovich, C.F. (2013). Muscle lipogenesis balances insulin sensitivity and strength through calcium signaling. J Clin Invest *123*, 1229-1240.

Lin, X., Chen, Z., Yue, P., Averna, M.R., Ostlund, R.E., Jr., Watson, M.A., and Schonfeld, G. (2006). A targeted apoB38.9 mutation in mice is associated with reduced hepatic cholesterol synthesis and enhanced lipid peroxidation. American journal of physiology. Gastrointestinal and liver physiology *290*, G1170-1176.

Lin, X., Ma, L., Racette, S.B., Anderson Spearie, C.L., and Ostlund, R.E., Jr. (2009). Phytosterol glycosides reduce cholesterol absorption in humans. Am J Physiol Gastrointest Liver Physiol *296*, G931-935.

Newberry, E.P., Xie, Y., Kennedy, S., Han, X., Buhman, K.K., Luo, J., Gross, R.W., and Davidson, N.O. (2003). Decreased hepatic triglyceride accumulation and altered fatty acid uptake in mice with deletion of the liver fatty acid-binding protein gene. J Biol Chem *278*, 51664-51672.

Odegaard, J.I., Ricardo-Gonzalez, R.R., Red Eagle, A., Vats, D., Morel, C.R., Goforth, M.H., Subramanian, V., Mukundan, L., Ferrante, A.W., and Chawla, A. (2008). Alternative M2 activation of Kupffer cells by PPARdelta ameliorates obesity-induced insulin resistance. Cell Metab *7*, 496-507.

Oh, J., Riek, A.E., Weng, S., Petty, M., Kim, D., Colonna, M., Cella, M., and Bernal-Mizrachi, C. (2012). Endoplasmic reticulum stress controls M2 macrophage differentiation and foam cell formation. J Biol Chem *287*, 11629-11641.

Oh, J., Weng, S., Felton, S.K., Bhandare, S., Riek, A., Butler, B., Proctor, B.M., Petty, M., Chen, Z., Schechtman, K.B., et al. (2009). 1,25(OH)2 vitamin d inhibits foam cell formation and suppresses macrophage cholesterol uptake in patients with type 2 diabetes mellitus. Circulation *120*, 687-698.

Riek, A.E., Oh, J., and Bernal-Mizrachi, C. (2013). 1,25(OH)2 vitamin D suppresses macrophage migration and reverses atherogenic cholesterol metabolism in type 2 diabetic patients. J Steroid Biochem Mol Biol *136*, 309-312.

Riek, A.E., Oh, J., Sprague, J.E., Timpson, A., de las Fuentes, L., Bernal-Mizrachi, L., Schechtman, K.B., and Bernal-Mizrachi, C. (2012). Vitamin D suppression of endoplasmic reticulum stress promotes an antiatherogenic monocyte/macrophage phenotype in type 2 diabetic patients. J Biol Chem *287*, 38482-38494.
Schneider, J.G., Finck, B.N., Ren, J., Standley, K.N., Takagi, M., Maclean, K.H., Bernal-Mizrachi, C., Muslin, A.J., Kastan, M.B., and Semenkovich, C.F. (2006). ATM-dependent suppression of stress signaling reduces vascular disease in metabolic syndrome. Cell Metab *4*, 377-389.
Tordjman, K., Bernal-Mizrachi, C., Zemany, L., Weng, S., Feng, C., Zhang, F., Leone, T.C., Coleman, T., Kelly, D.P., and Semenkovich, C.F. (2001). PPARalpha deficiency reduces insulin resistance and atherosclerosis in apoE-null mice. J Clin Invest *107*, 1025-1034.
Zhao, G., and Simpson, R.U. (2010). Interaction between vitamin D receptor with caveolin-3 and regulation by 1,25-dihydroxyvitamin D3 in adult rat cardiomyocytes. J Steroid Biochem Mol Biol *121*, 159-163.
Zinselmeyer, B.H., Dempster, J., Wokosin, D.L., Cannon, J.J., Pless, R., Parker, I., and Miller, M.J. (2009). Chapter 16. Two-photon microscopy and multidimensional analysis of cell dynamics. Methods in enzymology *461*, 349-378.